Materials Science and Engineering: C, 2013, Volume 33, Issue 8, Pages 4905-16.

ELECTROSPUN COMPOSITES OF PHBV, SILK FIBROIN AND NANO-HYDROXYAPATITE FOR BONE TISSUE ENGINEERING

Elena I. Paşcu, Joseph Stokes, Garrett B. McGuinness*

Centre for Medical Engineering Research, Dublin City University, Dublin, Ireland
School of Mechanical and Manufacturing Engineering, Dublin City University, Dublin, Ireland

Citation:

Paşcu EI, Stokes J, McGuinness GB. Electrospun composites of PHBV, silk fibroin and nano-hydroxyapatite for bone tissue engineering. Materials Science and Engineering: C. 2013 Dec 1;33(8):4905-16.

*Corresponding author at: Centre for Medical Engineering Research, School of Mechanical and Manufacturing Engineering, Dublin City University, Ireland. Tel.: +353 1 7005423

E-mail: garrett.mcguinness@dcu.ie (G.B. McGuinness)

Keywords:

Polyhydroxybutyrate-co-(3-hydroxyvalerate)

PHBV

Silk fibroin

Nanohydroxyapatite

Electrospinning

Bone tissue engineering

Abstract:

Electrospinning of fibrous scaffolds containing nano-hydroxyapatite (nHAp) embedded in a matrix of functional biomacromolecules offers an attractive route to mimicking the natural bone tissue architecture. Functional fibrous substrates will support cell attachment, proliferation and differentiation, while the role of HAp is to induce cells to secrete extracellular matrix (ECM) for mineralization to form bone. Electrospinning of biomaterials composed of polyhydroxybutyrate-co-(3-hydroxyvalerate) with 2% valerate fraction (PHBV), nano hydroxyapatite (nHAp), and *Bombyx mori* silk fibroin essence (SF), Mw =90KDa, has been achieved for nHAp and SF solution concentrations of 2 (w/vol) % each and 5 (w/vol) % each. The structure and properties of the nanocomposite fibrous membranes were investigated by means of Scanning Electron Microscopy in combination with Energy Dispersive X-ray Analysis (SEM/EDX), Fourier Transform Infrared Spectroscopy (FT-IR), uniaxial tensile and compressive mechanical testing, degradation tests and *in vitro* bioactivity tests. SEM images showed smooth, uniform and continuous fibre deposition with no bead formation, and fibre diameters of between 10-15μm. EDX and FT-IR confirmed the presence of nHAp and SF. After one month in deionised water, tests showed less than 2 % weight loss with the samples retaining their fibrous morphology, confirming this material biodegrades slowly. After 28 days of immersion in Simulated Body Fluid (SBF) an apatite layer was visible on the surface of the fibres, proving their bioactivity. Preliminary *in vitro* biological assessment showed that after 1 and 3 days in culture, cells were attached to the fibres, demonstrating retaining their morphology while presenting a flattened appearance and elongated shape on the surface of fibres. Young's modulus was found to increase from 0.7 kPa (±0.33kPa) for electrospun samples of PHBV only to 1.4kPa (±0.54 kPa) for samples with 2 (w/vol) % each of nHAp and SF. Samples prepared with 5 (w/vol) % each of nHAp and SF did not show a similar improvement.

1. Introduction

Bone is a complex and highly specialized form of connective tissue which acts as the main supporting organ of the body. It is hard and dynamic by its nature, with a unique combination of organic and inorganic elements embedded in a fibrous extracellular matrix (ECM), onto which cells attach, proliferate and differentiate [1]. When bone repair mechanisms fail, due to infection or defect magnitude, bone formation can be stimulated with the use of autologous bone grafts or donor allografts. However, autografts are associated with limitations such as donor site morbidity and limited availability, while allografts have the potential to cause an immune response and also carry the risk of pathogen transfer.

Bone tissue engineering has emerged as an alternative to these approaches [2]. One of its challenges is to mimic the architecture of the bone tissue while providing appropriate cues for cellular attachment, growth and proliferation, as well as the mechanical strength necessary to maintain their structural integrity during remodelling [3]. Together with judicious choice of biomaterial, the ability to electrospin nano and microscale fibres has greatly enhanced the scope for fabricating scaffolds that can potentially meet this challenge [4].

Electrospinning is a simple, cost effective and versatile method that can be used to produce fibrous structures with small diameters fibres with potential tissue engineering applications[5]. The process uses a high-voltage electric field to form solid fibres from a polymeric fluid jet delivered through a millimetre–scale nozzle. The electrospinning parameters (e.g., voltage, feed rate, needle tip to collector distance) can be varied in order to produce nanofibres with complex and unique three-dimensional shapes. Polymeric and composite solutions can be transformed into fibrous structures and, through adjustment of the process parameters; a wide range of properties can be tailored. The convenience of combining various materials in the electrospinning process makes it attractive for bone tissue

engineering. Furthermore, fibrous surfaces are associated with improved cell attachement by comparison with smooth surfaces [6- 8].

Natural bone extracellular matrix (ECM) consists of inorganic salts and collagen fibrils embedded in proteoglycans and organized in a three-dimensional porous network. While collagen can be extracted from animal tissue or produced using the transgenic method, both methods are expensive and the animal tissue extracted collagen may cause an immune response [1]. In order to mimic the fibrous structure of the ECM, care should be taken when selecting the most appropriate scaffold biomaterial, since its properties will determine the properties of the scaffold itself [10].

One of the materials of interest for tissue engineering applications is polyhydroxybutyrate (PHB) which can be produced by microorganisms *via* fermentation. It is a biodegradable and biocompatible polymer with piezoelectric properties (a property shared with bone) [11] and has been used in medical applications, such as scaffolds and drug delivery [12]. PHB homopolymers are highly crystalline, extremely brittle and relatively hydrophobic. On the other hand, the copolymers of PHB with polyhydroxyvalerate (PHV) are less crystalline and more readily processible [13]. Also PHB/PHV exhibits good oxygen permeability and its degradation products, such as 3-hydroxybutyrate, are normal mammalian metabolites [14]. Together with high biocompatibility, PHB-PHV polymers have degradation times much longer than many other biocompatible polymers, which may protect the mechanical integrity of the tissue/scaffold construct further into the bone remodelling phase [15]. It has been shown that degradation rate of PHBV can be readily adjusted by changing the copolymer composition and that PHBV forms with lower crystallinity have a higher degradation rate in aqueous media [16].

Hydroxyapatite (HAp), a major component of mineralised tissue, such as bone and teeth, has frequently found use in bioengineering, mainly as implant coatings, due to its

osteoinductivity [9]. At the same time, its brittleness and poor mechanical stability have limited its use on its own for the regeneration of non-load-bearing bone defects [10]. Hydroxyapatite is used to modify the mechanical properties of polymeric implants for certain medical applications. Nano sized particles of hydroxyapatite (nHAp) will have increased surface area and also have the ability to modify the absorption of chemical species, properties that can be used to promote cell activity and increase mineralization rate. Importantly, the incorporation of nano sized hydroxyapatite particles into a polymeric matrix can also improve the mechanical properties and support calcium and phosphate delivery after implantation [17, 18]. Composites of PHBV and HAp with partial biodegradability and high mechanical strength and osteoconductivity were reported to be suitable for fracture fixation [19].

Silk fibroin (SF), a protein extracted from the silk produced by culture silkworms and spiders, is composed of 17 amino acids. When appropriately purified, SF is non-toxic, non-immunogenic and has been demonstrated to support cell and tissue growth [20]. Due to several distinctive biological properties such as good biocompatibility, biodegradability, low inflammation reaction, no blood clotting effects and good mechanical properties, silk fibroin protein has been extensively studied as a promising materials for biomedical applications [21-23]. The electrospinning process has frequently been employed to investigate the creation of fibrous scaffolds for potential bone tissue engineering scaffold applications. Various nanocomposite fibres, such as PCL/$CaCO_3$ [23], HAp/gelatine [24], PLA/HAp [26-28] , PLA and triphasic HAp/collagen/PCL [29, 30] have been explored, with the intention of achieving better cellular adhesion, mineral formation and growth suitable for bone regeneration. Even though some of the synthetic polymers and their blends exhibit biocompatibility and adequate mechanical properties for load bearing applications (e.g. PCL, PLA, PMMA), novel biopolymer composites based on biodegradable and bioresorbable materials have received increasing interest over recent decades. The co-precipitation of HAp nanocrystals in soluble collagen has met with partial success in the fabrication of electrospun HAp–collagen

nanocomposites similar to the nanostructure of real bone, though with weaker mechanical properties [31]. On the other hand, carbonate-substituted HAp–chitosan/SF composites prepared using a co-precipitation method rather than electrospinning exhibited better compressive strength and cellular response [32]. Simultaneous gas-jet and electrospinning of composite solution containing hydroxyyapatite have been used to manufacture porous scaffolds suitable for bone regeneration [33, 34]. Other attempts at adding hydroxyapatite to the electrospun fibres have been made, either by soaking the fibrous polymeric matrix in Simulated Body Fluid (SBF) [35] or by co-precipitation and nucleation [36, 37]. PLGA/HAp fibrous composite scaffolds were also prepared, mainly used for drug delivery instead of bone repair [38- 40].

The objective of this preliminary study is to investigate the physical characteristics of nHAp embedded bacterial polyester fibrous scaffolds incorporating silk fibroin. In addition, 1 and 3 day *in vitro* biological evaluation of toxicity is presented, together with a qualitative assessment of cell adhesion. Silk fibroin is used to complement the matrix function, and to aid electrospinning of the solution. To the best of our knowledge, this is the first time these two natural polymers have been used together in electrospinning for bone tissue engineering applications. The specific aim of the study therefore is the development of tri-phasic PHBV/ nHAp/ silk fibroin (P/H/S) fibrous composites for bone regeneration scaffolds. The influence of the polymeric matrix materials, HAp particles and the fabrication conditions on the physical properties and biological toxicity will be critical to successful scaffold development.

In this study, novel nanocomposite fibrous membranes of nHAp, SF and PHBV have been electrospun, with two different concentrations of nano hydroxyapatite and silk fibroin. Polyhydroxybutyrate-co-(3-hydroxyvalerate) with 2% valerate fraction has been used as the polymeric matrix in which the other two phases have been incorporated.

2. Materials and methods

The electrospinning process allows production of fibres from different natural and synthetic polymeric solutions, and also from composite solutions. The first step taken in our research work was to prepare and electrospin a pure PHBV solution (P0). Once a suitable set of parameters (voltage, feed rate and needle tip to collector distance) for this solution was determined, composite blends (PHBV/ nHAp and PHBV/nHAp/SF) were prepared and used. The addition of nHAp to the PHBV solution changed its properties, making it more difficult to electrospin (non-uniform deposition of fibres was observed, as well as bead formation and electrospraying), while with the further addition of SF, electrospinning was readily initiated and deposited fibres were continuous and smooth.

2.1 Materials

Polyhydroxybutyrate-co-(3-hydroxyvalerate) with 2% valerate fraction (PHBV, M_W= 410.000 g/mol) was purchased from Good Fellow - UK; chloroform (CF) was purchased from Lennox -UK and nano size (< 200 nm) hydroxyapatite from Sigma Aldrich, Ireland. *Bombyx mori* silk fibroin essence (Mw= 90Da) was supplied by Huzhou Sunergy World Trade Co. Ltd (Huzhou, Republic of China).

2.2 Preparation of the composite solution

HAp nanoparticles were sonicated in chloroform for 15 min, prior to adding the PHBV powder. Then, the PHBV was dissolved in chloroform by continuous stirring at 70 °C for 30 min (15g of polymer in 100ml of solvent). The *Bombyx mori* SF was added last. This paper presents results for the polymeric PHBV matrix (P0) and two composite combinations (P2 and P5) (Table 1).

Table 1 Composite solutions and codes

PHBV	**nHAp**	**SF**	**Code**
15%PHB98-PHV2	0%	0%	PO
15%PHB98-PHV2	2%	2%	P2
15%PHB98-PHV2	5%	5%	P5

2.3 Electrospinning of composite membranes

The pure polymeric (P0) or composite (P2, P5) solution was placed in a 10-mL plastic syringe with an inner needle diameter of 0.514 mm. For all experiments the syringe was placed horizontally and membranes were collected on square aluminium plates (5 cm x 5cm, 0.2mm thickness) using a positive voltage connected to the needle and a negative voltage connected to the collector plate. The voltage used for both the positive and negative electrode was of 15kV (P0) and 10kV (P2, P5) *via* a Gamma High Voltage Research power supply. The collection time was of 20 minutes and the feed rate was 2ml/h (P0) or 5 ml/h (P2, P5). The distance between the syringe needle and the aluminium plate collector was kept constant (d=15cm).

2.3 Characterisation of the electrospun nanocomposite membranes

The morphologies of the electrospun fibrous scaffolds were examined using Scanning Electron Microscopy (SEM, Zeiss EVO LS15) with image analysis and qualitative EDX capabilities. The spot analysis and element mapping of energy-dispersive x-ray spectroscopy were used to confirm the elements present on the electrospun fibres while assessing the distribution of these particles. Samples were first coated with a 3-5 nm thin layer of gold using a Edward Pirani 501 Scancoat six sputter coater and analyzed at an accelerated voltage of 10-20kV.

Fibre diameters were measured with the help of image analysis and processing software (Image J 1.44p, National Institute of Health, USA), using the SEM images, while the thickness of samples was measured using a Mitutoyo microscope (Mitutoyo Corporation, Japan).

Porosity measurements employed the use of helium pycnometer (Micrometirics, AccuPcyc 1330, USA) and were calculated from replicate measurements of volume and density, using the following formula:

$$\varphi = (1 - \rho_b/\rho_g) \times 100 \qquad (1)$$

where ρ_b is the bulk density and ρ_g is the grain density.

Membrane wettability was assessed using static advancing contact angle measurement The method used for our tests was the sessile drop technique, using ArtCAM 130 MI BW monochrome camera, and FTA200 contact angle analyser software. Contact angle evolution was analysed for 3 s. Before conducting the measurements the flat samples were cut and cleaned with an air pistol, in order to remove any impurities.

Differential thermal and thermogravimetric analysis were used to thermally characterise the composite sample. For this a DTA/TGA- Simultaneous Thermal Analysis (STA), PL Thermal Sciences Ltd., UK was used. The analysis was carried out by linearly increasing the temperature by 20ºC/min from 20ºC to 600°C in a nitrogen atmosphere. The total weight of the specimen for each thermal analysis was 20 mg. The chemical bonding

structures present in the fibre were analysed using Fourier Transform Infrared Spectroscopy (Spectrum GX FT-IR) equipped with an ATR accessory Horizontal Attenuated Total Reflectance (HATR) with zinc selenide (ZeSe) crystal. A mixture of the powder to be tested (2 mg) and potassium bromide salt (200 mg) was ground in a marble mortar for 10 minutes, to avoid scattering from large crystal. The ground powder was then added into a die and pressed at 12 kPa for 15 min to form a translucent pellet, which allows the IR beam to pass through it.

Raman scattering measurements were used to determine the presence of apatite layer formed on the surface of the fibrous samples after one month in SBF. Measurements were performed using a HoribaYvon LabRAM 800 HR. The parameters used for the spectra were as follows: excitation laser 784.7 nm diode laser, grating 600 g/mm, objective 50x Fluortar, and 6 accumulations at an exposure time of 4 seconds.

For mechanical characterization of the composite samples tensile and compression tests were run, under dry conditions at 22ºC. For tensile tests, dog bone-shaped samples (40 mm gauge length × 10mm width) were cut by die-cutting from the flat electrospun membranes. Young's modulus of the porous fibrous polymeric and composites samples were determined using a Zwick/Roell Z500 N universal testing machine equipped with a 20N load cell (Zwick GmbH, Ulm, Germany). The results were plotted with Test Xpert II (Zwick GmbH, Ulm, Germany). Samples were tested up to failure. For each composition 6 samples were tested and results were expressed in terms of mean average and standard deviation. Statistical significance was analysed.

For mechanical evaluation under compression, sets of 6 electrospun fibrous cubes were tested for each composite type using a Zwick/Roell Z500 N universal testing machine equipped with a 5kN load cell (Zwick GmbH, Ulm, Germany). Electrospun flat membranes collected over a period of 20 min were folded and cubes of 1cm x 1cm were cut. Constructs thickness varied from 0.25mm - 0.3mm for the P0 to 0.36mm - 0.4 mm for P2 and P5

composites. The cubes were compressed at a rate of 2mm.min^{-1} until 80% strain was reached. Results are expressed in terms of the secant modulus for a stress of 0.4 MPa.

In vitro studies to assess the pH and conductivity change of the polymeric and composite samples were carried out for a period of 4 weeks. Additionally pH and conductivity changes were recorded. Triplicates of 1cm x 1cm fibrous samples were cut, weighed and immersed in 50ml of deionised water. In order to investigate the true pH changes over time a non-buffer solution that will not mask any pH changes over time was the chosen aging media for the test. At regular intervals, samples from buffer were removed, extensively rinsed with distilled water and dried under vacuum room temperature and weighed. The pH and conductivity values were recorded every day.

The bioactivity test was carried out using the standard acellular *in-vitro* procedure as described by Kokubo [41]. The nanocomposite fibrous pieces (1cm x1cm) were immersed in 100ml of acellular SBF (pH 7.30 at 37°C) in flasks. The flasks were placed in a water bath at 37°C. The SBF solution was refreshed twice a week. The samples were removed from SBF solution after 7, 14, 21 and 28 days. After removal from the SBF fluid, the samples were gently rinsed with deionised water and left to dry at room temperature for 24h. Apatite formation was assessed using SEM/EDX and FT-Raman analysis.

2.4 Statistical Analysis

All results were expressed as means and standard deviations. Statistical significance of the differences among polymeric scaffolds (control) and composite samples was determined using the Student's t test.

2.5 Qualitative preliminary biological evaluation of the obtained materials

Cell culture

Human osteoblasts (HOB) (PromoCell, Germany) were used for preliminary evaluation of cell behaviour on the obtained scaffolds. The cells were cultured in PromoCell growth medium, supplemented with 10% heat inactivated foetal calf serum (FCS, PromoCell, Germany), penicillin-streptomycin 10ml/L (Sigma-Aldrich, Ireland) and amphotericin 320 µl/L (Sigma-Aldrich, Ireland) under standard cell culture conditions (37ºC, 5% CO_2). The medium was changed every day. For the biological study, cells attached to the culture flask were washed with HEPES-BSS (PromoCell, Germany), trypsinized (trypsin-EDTA; PromoCell, Germany), centrifuged at 300rpm for 3min, and re-suspended in the growth medium. Cells were counted with a haemocytometer and seeded on the scaffolds at a density of 50,000 viable cells per sample. Passage number 4 was used in this experiment. Cells on tested materials were incubated in standard cell culture conditions for 1 and 3 days. For the initial testing, the material with the highest content of the nHAp and SF additives has been chosen (P5) and unmodified material (P0) served as a reference sample.

Cell morphology

To assess cell morphology Scanning Electron Microscopy (SEM) was used. At the evaluation periods (1 or 3 days), osteoblasts on the scaffolds were fixed using a solution containing 2 vol% glutaraldehyde (Sigma-Aldrich, Ireland) in PBS (Sigma-Aldrich. Ireland) dehydrated in ethanol with sequential concentration, treated with hexamethyldisilazane (Fluka, Ireland) and dried in air. Samples were then sputtered with a 3-5 nm thick gold layer and observed, using a Scanning Electron Microscope (Leo 440, Stereo Scan), operated at 5.0 kV.

Cell viability and spatial distribution

The cell viability and spatial distribution within the obtained scaffolds were evaluated in cells stained with LIVE/DEAD Kit (Invitrogen, USA). Briefly, on the day of experiment HOB were washed twice in PBS and stained using 2 μM calcein and 4 μM Ethid-1 in PBS to observe live and dead cells respectively. Images were captured by a Nikon DS-U2 camera attached to the Nikon T*i*-E epifluorescent microscope, at 10× magnification, using the associated Nikon NIS-Elements software.

3. Results and discussion

3.1 Fibres morphology, structure and wettability

On a macroscopic scale, the electrospun polymeric sample of P0 exhibited a smoother surface compared with the tri-phasic membranes (P2 and P5) which both revealed macropores and higher irregularities on the surface. The SEM analysis showed that the fibres are randomly aligned, which is attributable to continuous deposition (no breaking was observed for individual fibres during electrospinning). Furthermore, these single fibres presented smooth surfaces without bead formation (Fig. 1). EDX results confirmed the elements calcium and phosphate were not present in P0 samples, whereas they were present in the P2 and P5 fibres (Figs. 1 and 2). The element mapping analysis revealed a uniform distribution of the elements on the nanofibrous membranes (Fig. 2). In Fig 2-A, only C and O elements can be detected, confirming the polymeric sample's composition (P0), while in Fig. 2-B and C white green dots corresponding to Ca and P elements are present, confirming the ceramic phase addition. These dots indicate that the nHAp phase is distributed on the mapping area, thus present on the fibrous structure. The DTA curve (Figure 3) also evidenced a ~ 12 % weight residue assumed to be the ceramic phase. This confirmed that the nHAp particles were incorporated within the composite fibres. The mono-phasic fibres measured 10-15μm in diameter, while the tri-phasic fibres were 13-20 μm in diameter (n = 20,

$p<0.001$) (Table 1). The fibre diameter was slightly increased for the tri-phasic composites and this could be attributed to the presence of nano-hydroxyapatite particle agglomerations within the polymeric fibres. It should be noted that the diameters obtained are not the smallest possible; they represent values that were found to produce the most consistent and uniform fibrous membranes. The parameters used for the composite samples (P2 and P5 respectively) were: feed rate = 5ml/h, syringe needle to collector plate distance = 15cm, positive and negative electrodes voltage= 10kV. For the pure polymeric solution collection (P0), feed rate was 5ml/h, syringe needle to collector plate distance=15cm, positive and negative electrodes voltage=15kV. The collection time was of 20 minutes for each of the samples.

It can be seen from Table 1 that the electrospun P0 has a relatively hydrophilic surface. Further, when adding silk fibroin essence and nHAp, there is a significant increase in the average contact angle ($p< 0.05$) even though the addition of silk fibroin essence would be expected to increase the hydrophilicity. This contradictory effect could be attributed to the rugosity variation of the composite samples (P2, P5) compared to the pure polymeric samples (P0) or the presence of hydroxyapatite on the fibre surface as proved by the EDX analysis [42,43]. In addition, the observed decrease in wettability of the composite samples could be the result of a change in porosity associated with the SF and nHAp additives, as reported in Table 1. Furthermore, a small but significant change in contact angle ($p<0.05$) values has also been observed between P2 and P5 samples, that may be due to sample composition and rugosity changes.

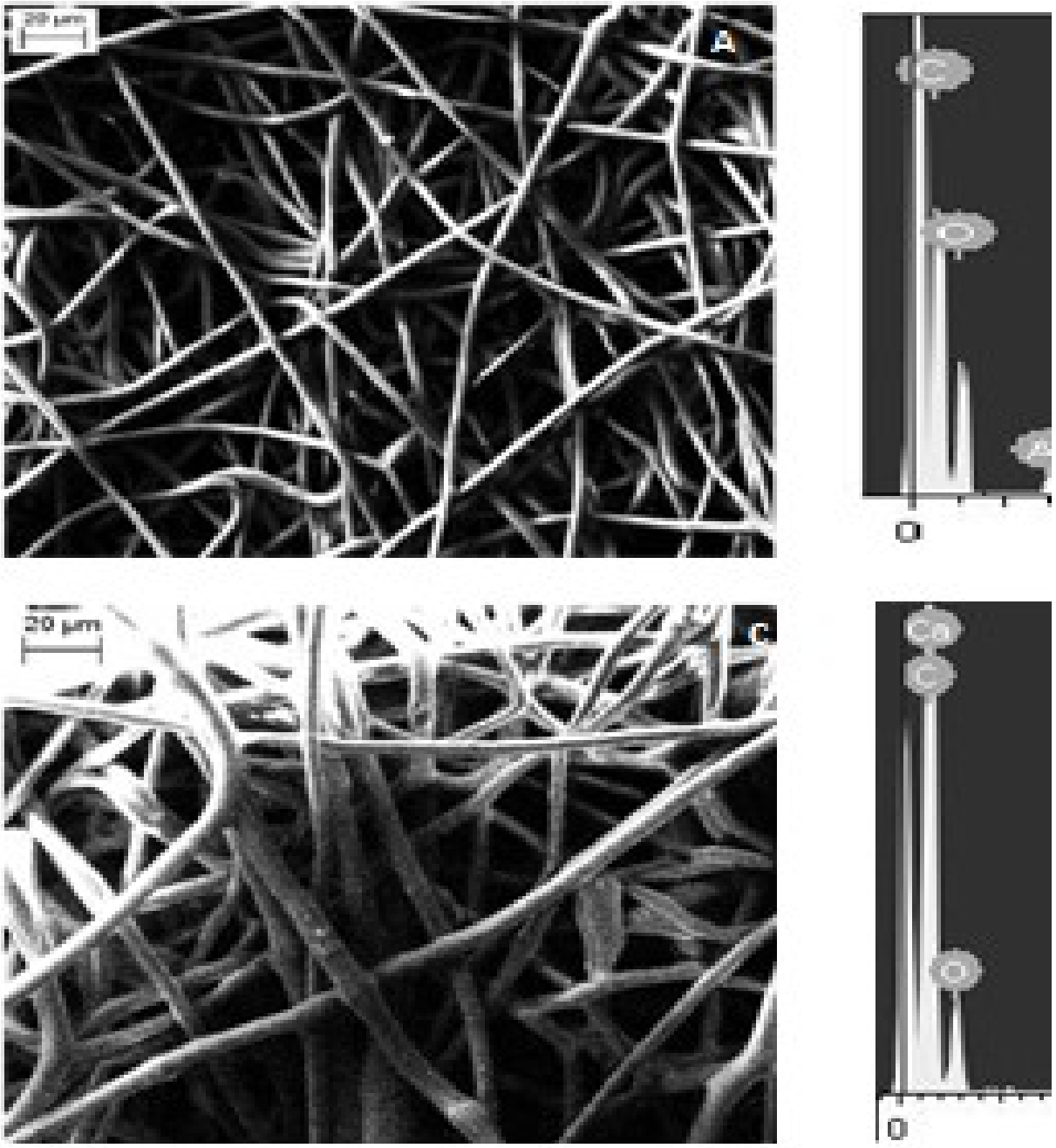

Figure 1 SEM/EDX images of (A/B) PO, (C/D) P2 and (E/F) P5 electrospun membranes

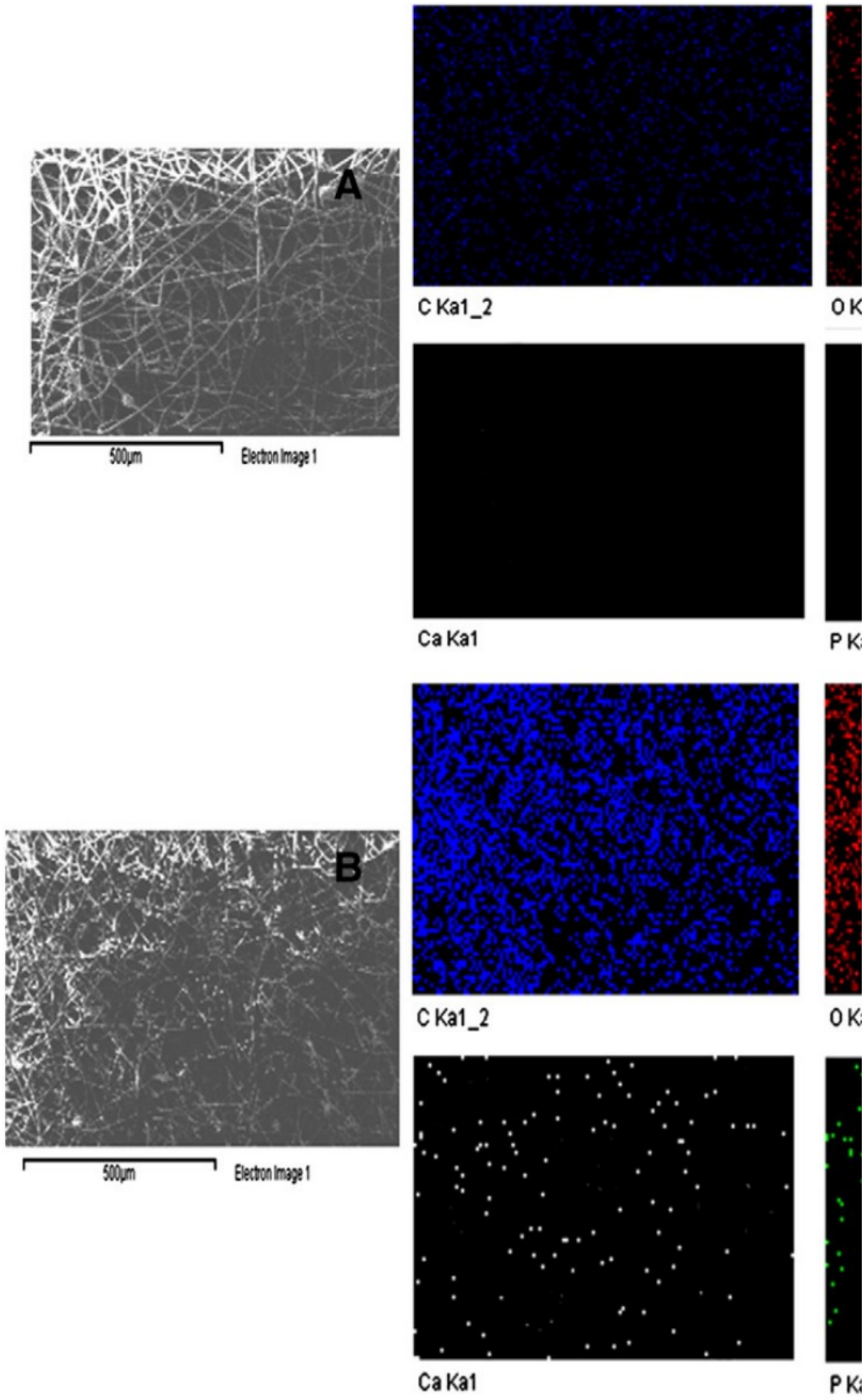

Fig 2.A. EDX element mapping analysis of P0 fibrous membranes (500 μm scale bar applies to all images). B. EDX element mapping analysis of P2 fibrous membranes (500 μm scale bar applies to all images). C. EDX element mapping analysis of P5 fibrous membranes (500 μm scale bar applies to all images).

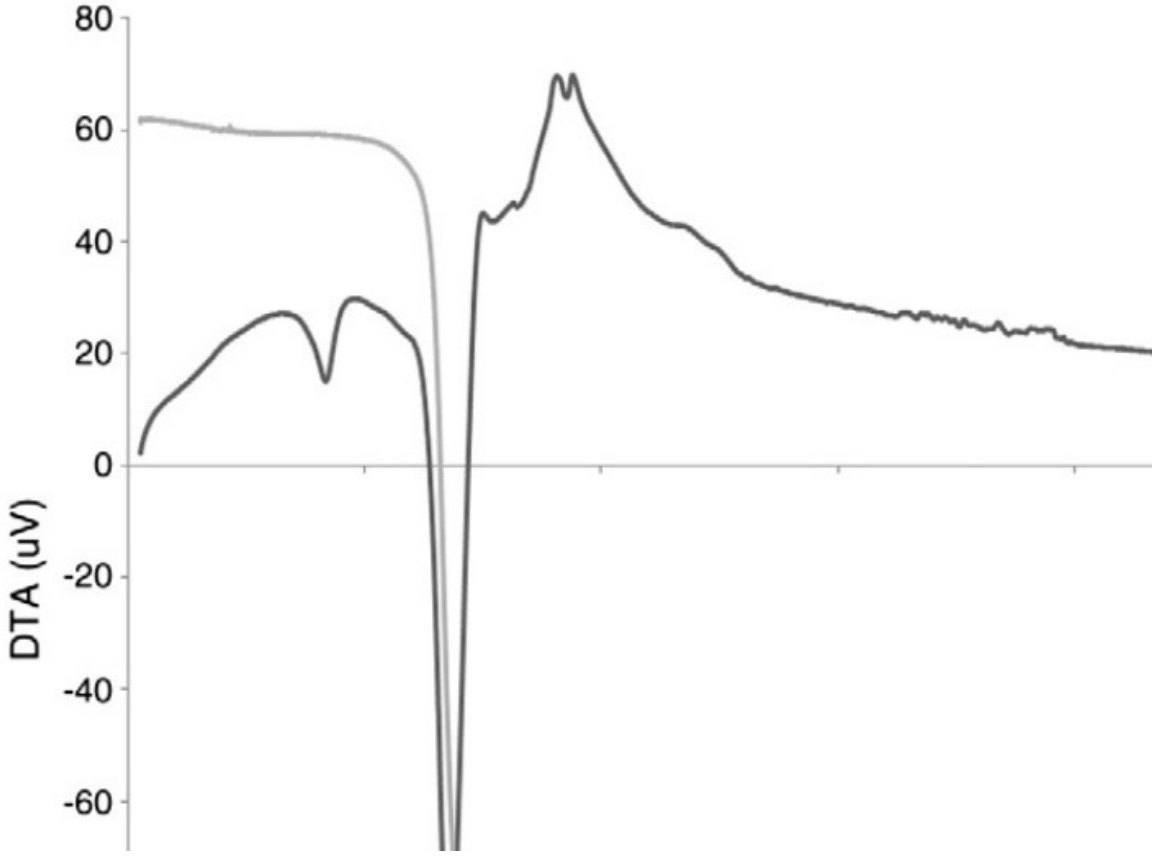

Fig. 3. TGA/DTA analysis of P2 composite

Significant porosity difference was found between the polymeric P0 samples and each of the two types of composite sample, with values of 75% for P0 and 70%-72% for P2, P5 ($p<0.05$, Table 2). Trabecular bone exhibits a porosity ranging anywhere from 50% to 90% [44]. Furthermore no significant difference in porosity was found between the two composite sample types (P2 and P5). This change in porosity could be attributed to the slight change in fibre diameter due to the presence of nano hydroxyapatite particles within the fibres [45]. Further, since fibre alignment control was not a goal of this preliminary stage of research, the random deposition could have been another factor for the change in porosity.

3.2 FT-IR spectra analysis

Fig 4 presents the FT-IR spectra of PHBV, nHA_P, SF powders and the P2 electrospun fibrous composite sample. The FT-IR characteristic bands for polyhydroxybutyrate are: C=O stretching at 1720 cm^{-1}, -C-O-C- stretching vibration at 800-900 cm^{-1} and an antisymmetric –C-O-C- stretching band at 1060-1150 cm^{-1}. Because the polymer used in this research contained a 2% valerate, the specific bands for the pure polyhydroxybutyrate were slightly changed, but they were still found in the raw powder. The characteristic bands for the nHAp powder are: OH stretching vibration at 3600 cm^{-1}, antisymmetric v3 and symmetric v1 P-O streching vibration (PO_4^3 bands) located at 1033 cm^{-1} and 962 cm^{-1} , and were confirmed to be present in the ceramic powder [46-48]. Also v2 and v3 modes of CO_3^{2-} at 870 cm^{-1} and 1400-1500cm^{-1} indicate absorbed H_20 while v4 O-P-O bending vibration should be between 600 - 550cm^{-1}.

Silk fibroin's characteristic bands are identified as amide A and amide I, amide II, and amide III [49, 50]. Amide A was found at 3294 cm^{-1} and it represents the –N-H stretching vibration. Amide I can be found between 1500-1600 cm^{-1}, amide II at 1380-1400 cm^{-1} and amide III at 1375 -1390 cm^{-1}. The three amides are related to the carbonyl -C-O- stretching mode, combination peak of the main N-H in plane bending, C-H stretching vibration, coupled peak of the main C-N stretching and the –N-H in plane bending vibration [49, 50]. The spectra of the composite P2 and that of the P0 revealed several common peaks, since the matrix was the same. These absorption peaks were the symmetric stretching vibration of C–CH_2 at 2845 cm^{-1}, the carbonyl peak at 1647 cm^{-1}, the methyl peak at 1385 cm^{-1} and the stretching vibration of C–O at 1210 cm^{-1}.The FT-IR analysis of the composite revealed the presence of the three amides, characteristic for the silk fibroin and also the PO_4^3 vibration bands v_1 and v3 of the hydroxyapatite. As can be observed in Fig. 4, the positions of the amides shifted and the vibration intensity apparently decreased with the addition of hydroxyapatite. The Ca^{2+} presence forced the –C-O and –N-H groups from the silk fibroin

molecule to be absorbed by the hydroxyapatite solution. The PO_4^3 vibration bands were found at 1030 cm^{-1} and 987 cm^{-1}, with decreased vibration intensity. No additional peaks, other than those corresponding to the PHBV, SF and nHAp were found, which indicates that there was no chemical bonding between the ceramic particles and the polymeric matrix.

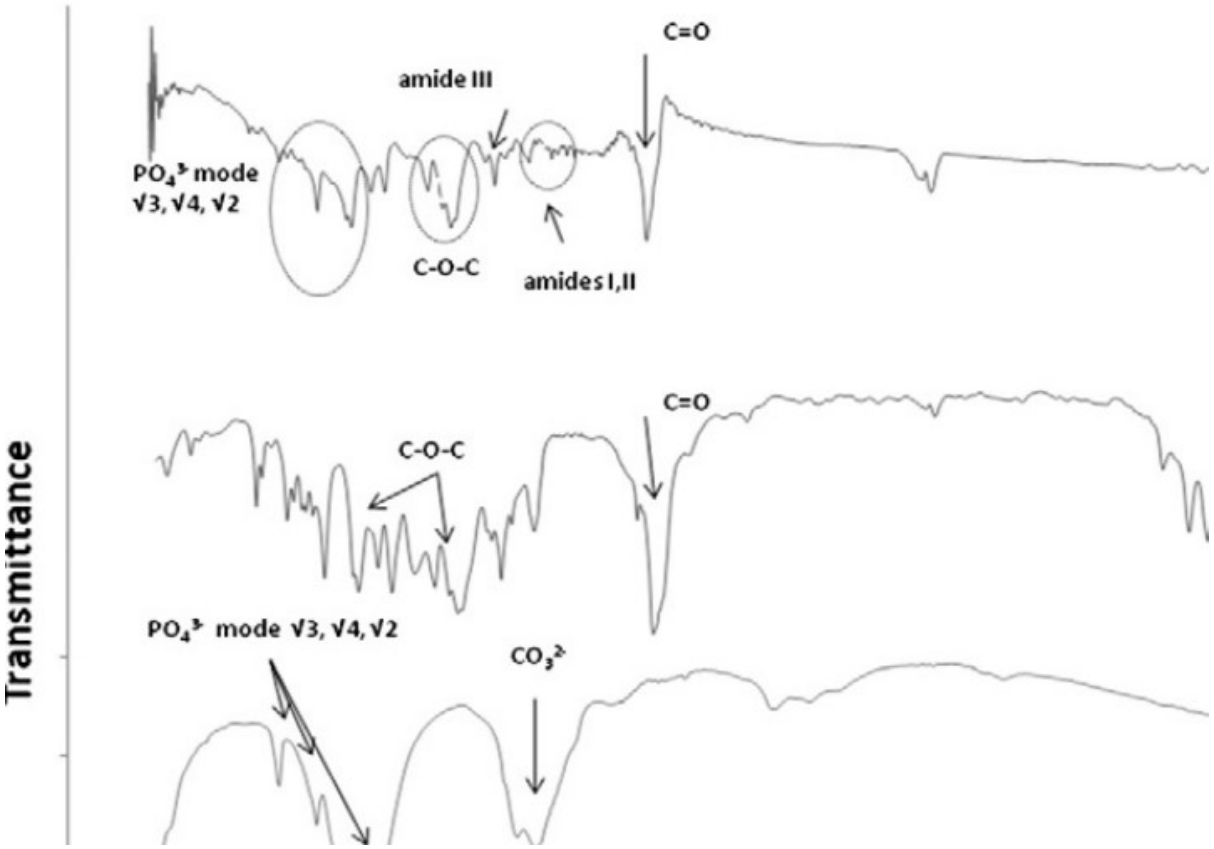

Fig.4. FT-IR spectra of PHBV, nHAp, SF powders and P2 composites

3.3 Conductivity and pH measurement

As seen in Figs 5 and 6, the pH and conductivity measurement tests were carried out for a period of one month. Samples of P0, P2 and P5 were cut into 1cm x 1cm pieces, weighed and immersed in deionised water at 37°C in a water bath (n=3). The deionised water was the chosen aging media as opposed to the phosphate buffer, as this will not mask any pH changes that might not be recorded when using the PBS solution.

SEM images were taken prior to and after the one month degradation test, for comparison reasons. Fig. 7 shows the morphology of the P2 fibrous nanocomposite sample after four weeks degradation and gives evidence that the fibrous structure has retained its porous structure with the fibres slightly swollen. The pH values stayed between 6.8 - 7.4, and the variations may be attributed to the difference in composition of the three samples. The conductivity results evidence a continuous release of ions from the samples, with a constant degradation rate for all the composite formulations (Table 2). Furthermore the random nature of the fibre deposition and the arrangement of the nHAp particles with respect to SF macromolecules within the fibres may have influenced the rate of degradation. The P2 electrospun membrane seems to have exhibited the fastest degradation rate during *in vitro* degradation with pH values changing from 7.2 to 6.8 at day 14. P0 and P5 samples degraded slower when compared to the P2 membrane, based on the corresponding pH values of 7.3 (PO) and 7.4 (P5) respectively at day 21.

Table 3 Conductivity results at day 1, 7, 14, 21 and 28 for PO, P2 and P5 samples

	CONDUCTIVITY RESULTS (µS)					
DAY	**PO**	**SD**	**P2**	**SD**	**P5**	**SD**
1	55.7	4.9	80	52.0	71	5.2
7	82	0	133	88.3	80	4.4
14	125	0	205.7	140.6	101.3	19.6
21	143	0	252.3	189.4	103.7	20.2
28	170	0	270.3	173.8	124.5	50.7

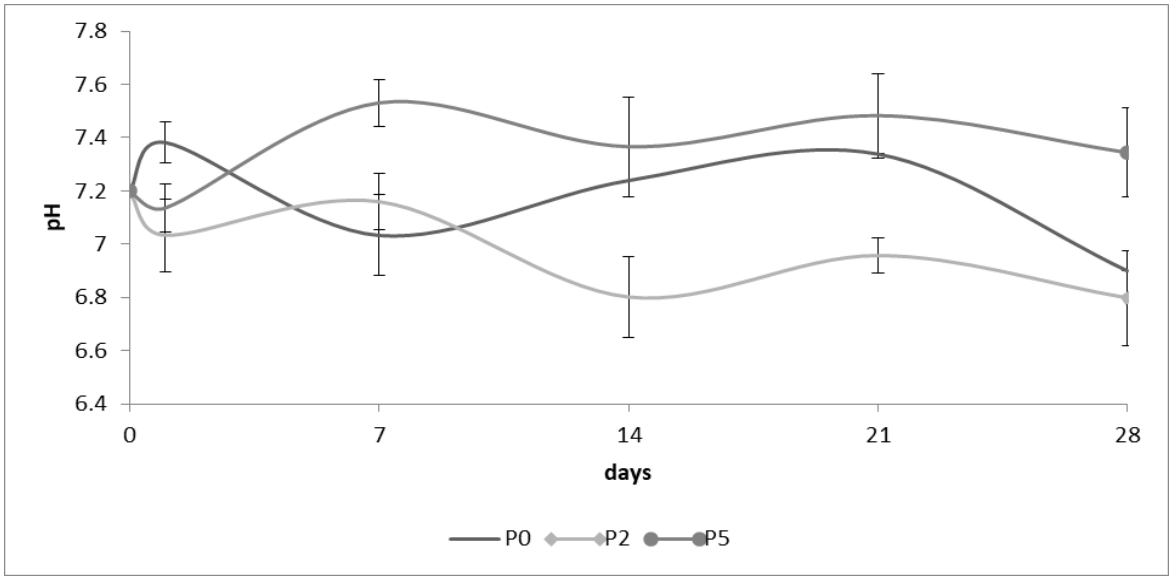

Fig. 5. pH measurements over one month period for P0, P2 and P5 composites samples (n =3)

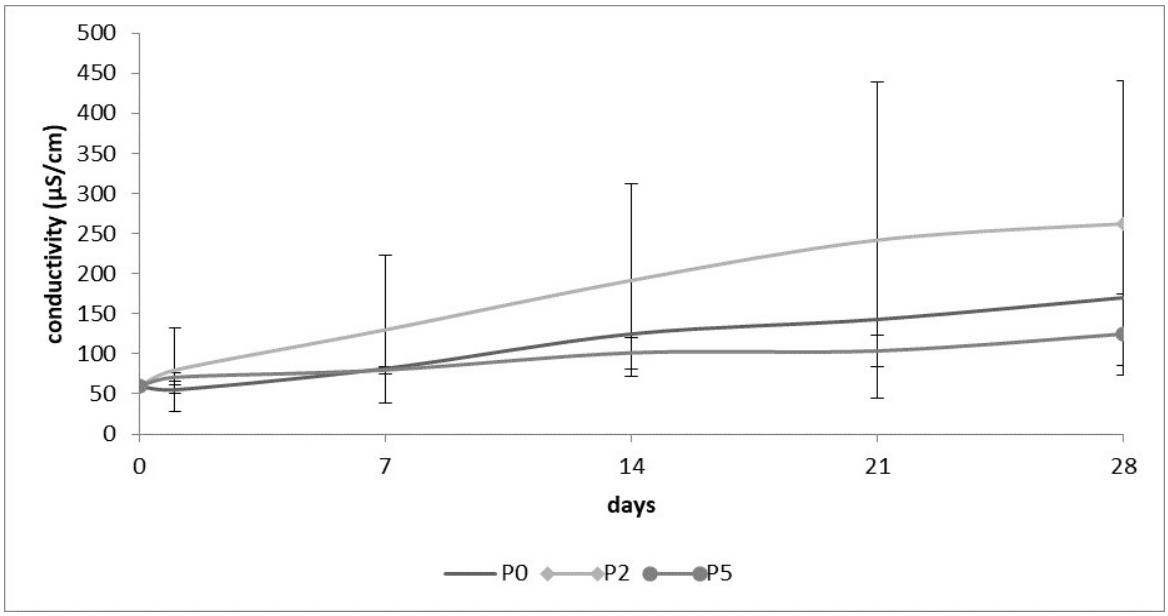

Fig. 6. Conductivity test run for one month period of (A) P0, (B) P2 and P5 composites samples (n =3)

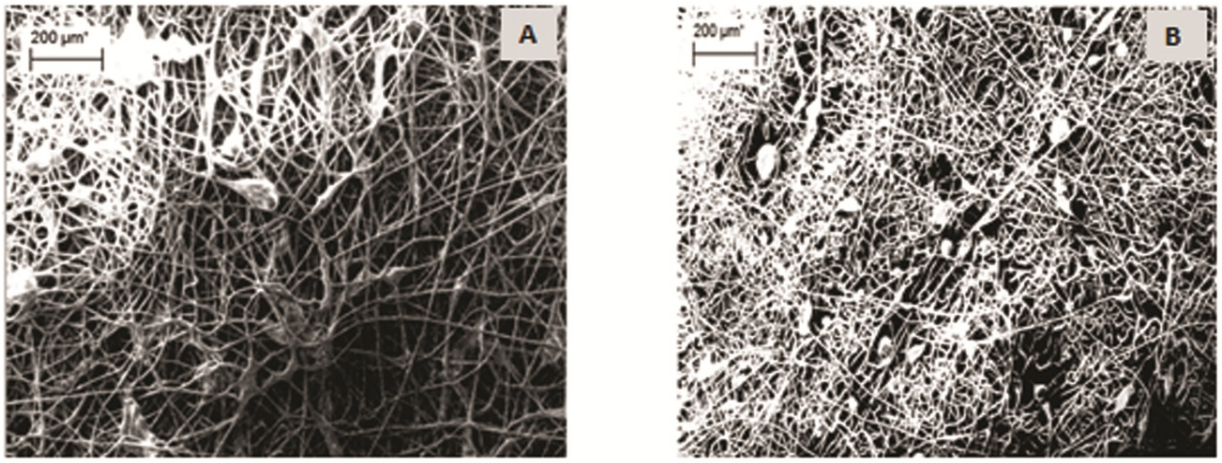

Fig. 7. SEM morphology of P2 sample (a) prior to and (b) after a 1month degradation test (20 x)

3.4 Mechanical properties of PHBV and composite electrospun matrices

Tensile tests were applied to P0 PHBV electrospun samples, as well as to the P2 and P5 composite samples with 2wt% and 5 wt% of nHAp and silk fibroin in the PHBV matrix.

The Young's modulus (Table 1) of the composite fibres decreases with increased content of nHAp and SF. This could be attributable to a lack of sufficient interfacial interaction between the PHBV matrix and the nHAp or SF phases respectively. The presence of polar groups on the hydroxyapatite particles and the abundant moderate polar groups in the chemical makeup of PHBV lead to an expectation of some interfacial interaction between the two, although from the FTIR analysis, no chemical or hydrogen bond interactions between the moderately polar groups of the two components were observed. [51]. According to the results the P2 composite samples revealed increased Young modulus when compared to the pure polymeric sample (control). The addition of 2% nHAp and silk fibroin phases had significantly improved the tensile properties of the P2 composite, although this increase was not found for the 5 wt.% nHAp and silk fibroin samples.

The compressive mechanical properties were also measured for the P0 PHBV electrospun matrix and for the P2 and P5 composite samples. The secant modulus at 0.4 MPa stress is shown in Fig. 8. The secant modulus is useful in describing the behaviour of materials which exhibit little or no linear behaviour. It was observed that an increased in ceramic concentration caused the modulus to decrease from 3.32 MPa for P0 to 0.48 MPa for the P5 composite. The prepared scaffolds did not manifest a critical stress under compressive loading, but a continuous increase of the load due to the progressive porosity reduction. The compressive mechanical properties of the composites are comparable to the low limit of some load-bearing tissues. Kurkijarvi *et al.* measured elastic and dynamic moduli of full-thickness, cartilage-bone cylinders of human (nonarthritic) knees to range from 0.15 to 2.14 MPa and 0.8–15.58 MPa [51]. Even so it is widely accepted that it is not essential for the scaffold to

have the same mechanical strength of the natural bone, however adequate mechanical properties are necessary for correct manipulation and positioning of the scaffolds.

3.5 'in vitro' bioactivity test

Fig. 9 shows the SEM images of electrospun fibrous membranes before and after 28 days in 1 x SBF. At day 0 in SBF no visible apatite crystals are present. However, after 28 days in SBF, a precipitated dune-like apatite layer made of spherical Ca-P particles was visibly covering the composite fibres as shown by the SEM analysis. EDX results proved that the white layer formed on the surface of the fibres consists of Ca^{2+} and P, with a ratio Ca/P of 1.75 (image included as supplementary material). Results from EDX analysis revealed the gradual development of apatite on the surfaces of the fibrous specimens after immersion for various times in SBF. Furthermore, the EDX analysis revealed the presence of Cl^- and Na^+ traces on the surface of the fibres, elements that originate from the SBF solution. The apatite phase was also identified on the Raman spectra (Fig. 10) with a characteristic peak at 960 cm $^{-1}$, due to the *v*1 PO_4^3mode and a strong band at 1035 cm^{-1} and 1076 cm^{-1} corresponding to the symmetric stretching vibration (PO_4^{3-} *v*3). In addition, three other PO_4^{3-} modes are present in the region of 450-400 cm^{-1} (PO_4^{3-} *v*2) and 610-579 cm^{-1} (PO_4^{3-} *v*4) [52,53]. One supplementary table summarizes the Raman peak positions and their assignments. Furthermore the presence of carbonate group on the spectra was confirmed from the molar Ca/P ratios which had values corresponding to non-stoichiometric biological apatite. [54, 55] This *in vitro* test shows that the composite is bioactive, and has the potential to initiate bone formation.

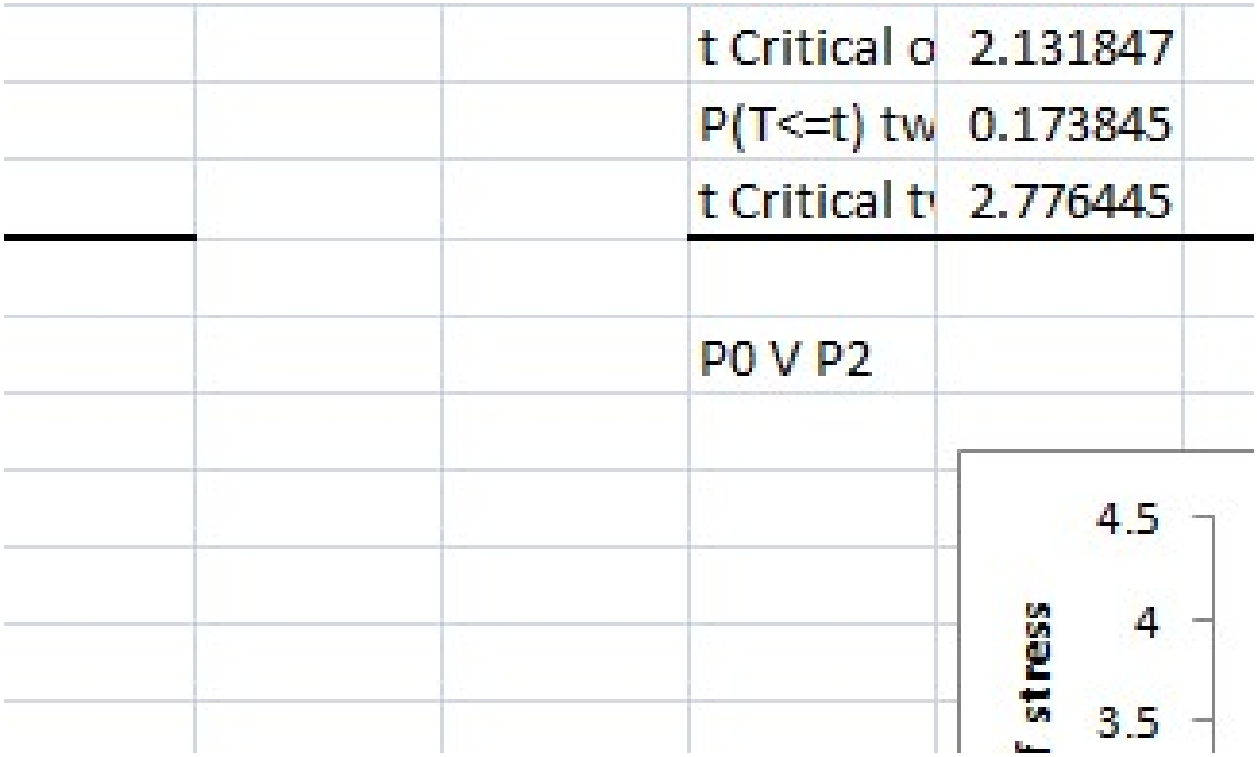

Fig. 8. Secant compressive modulus for three-dimensional electrospun composite blocks ($p<0.05$)

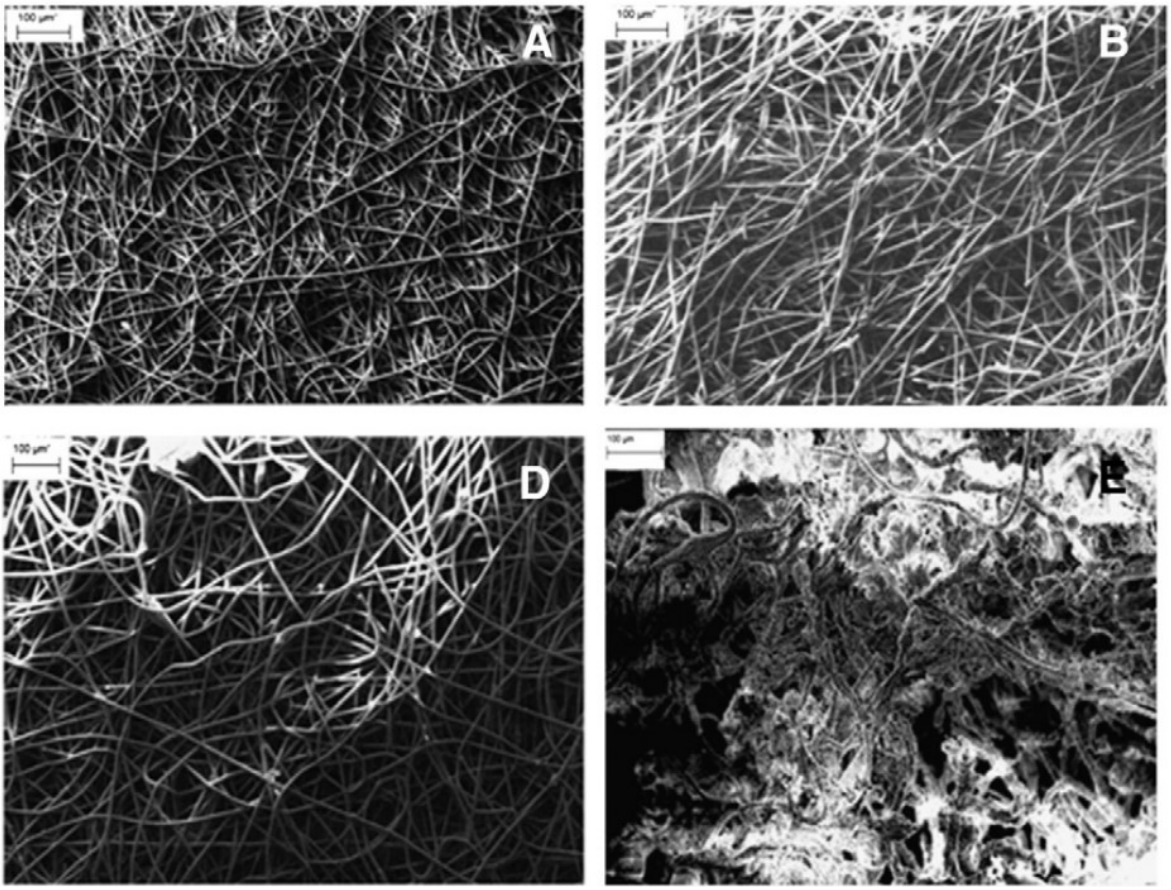

Fig. 9. SEM/analysis of electrospun samples, soaked in 1 x SBF, at 37C for 0 days, 100x (A) P0, (D) P2, (G) P5 and 28 days (B,C) P0, (E,F) P2, (H,I) P5 (B, E and H at 100x; C, F and I at 300x).

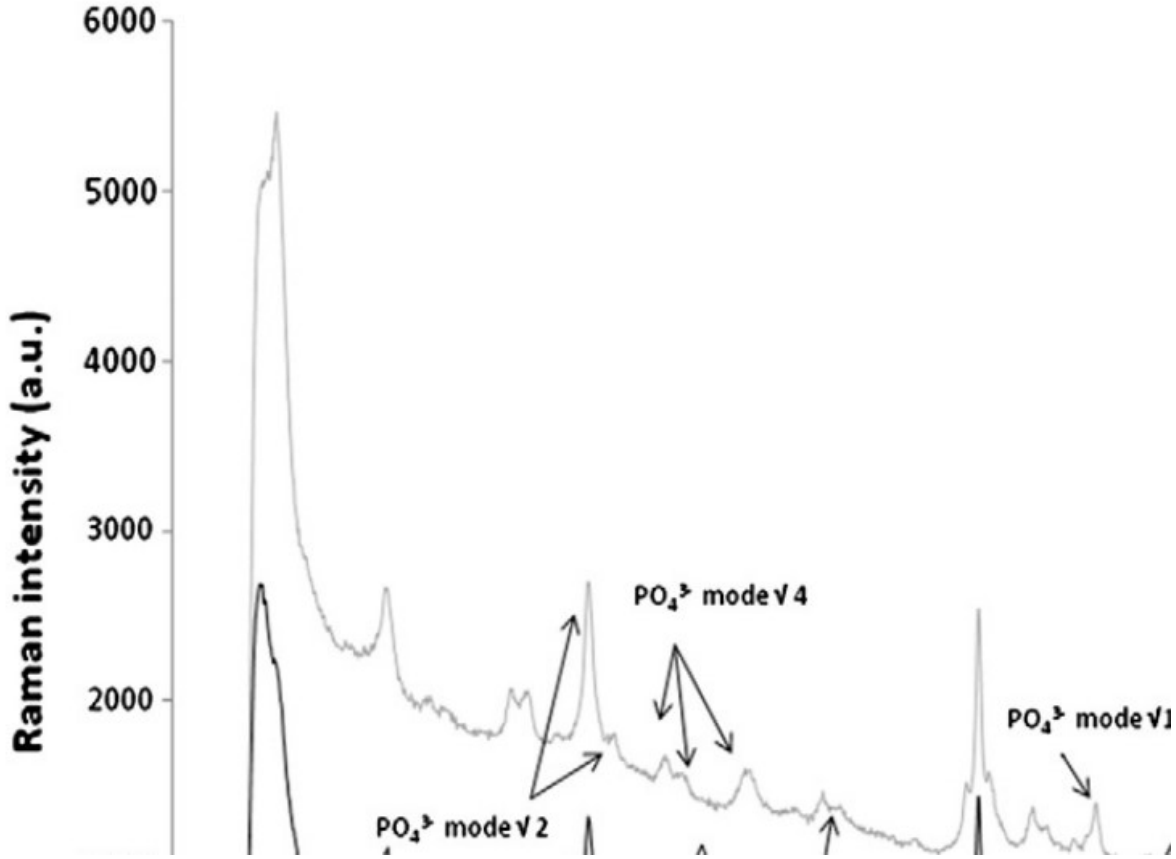

Fig. 10. Raman spectra of P2 composite before immersing in SBF and after 28 days in SBF.

3.6 Biological evaluation

As a prerequisite for the cell growth *in vitro*, a surface must support cell adhesion and spreading thus proving to be non toxic for the cellular entities [56]. A preliminary qualitative biological study performed on the scaffolds showed that attachment and growth of HOB cells was supported and the cells maintained their morphology. The control for this observation was the cells cultured on the polymeric matrix (P0) which has been shown in the past to support osteoblasts attachement and growth [57,58] Microscopy-based observations (SEM and fluorescent microscope) showed that the same trend was observed for modified (P5) and unmodified (P0) material. After 1 and 3 days of experimental testing, cells were attached to the fibres, demonstrating similar morphology with a flattened appearance and elongated shape on the surface of fibres (Figures 11 and 12). Additionaly LIVE/DEAD staining showed no cytotoxic effect of the tested materials on HOB cells. The cells were able to penetrate cavities between fibres and no significant difference in their behaviour was observed between

the test sample and control, despite the difference in the material composition and morphology. Figure 12 (A), shows that after 1 day of culturing there were single dead cells visible in the control material (red colour indicated by the yellow arrow). This can be associated with the process of cells seeding rather than with the material related cytotoxicity, as after 3 days of experiment (Figure 12 B, D) no more dead cells were observed on all tested materials. It can be seen that after 1 day, elongated and single round cells are visible while after 3 days all cells are elongated and well distributed within the scaffolds structure. Furthermore after 3 days in culture cells cell density on the surface of the sample seems to have decreased and this can be attributed to cells penetrating the scaffold's fibrous network.

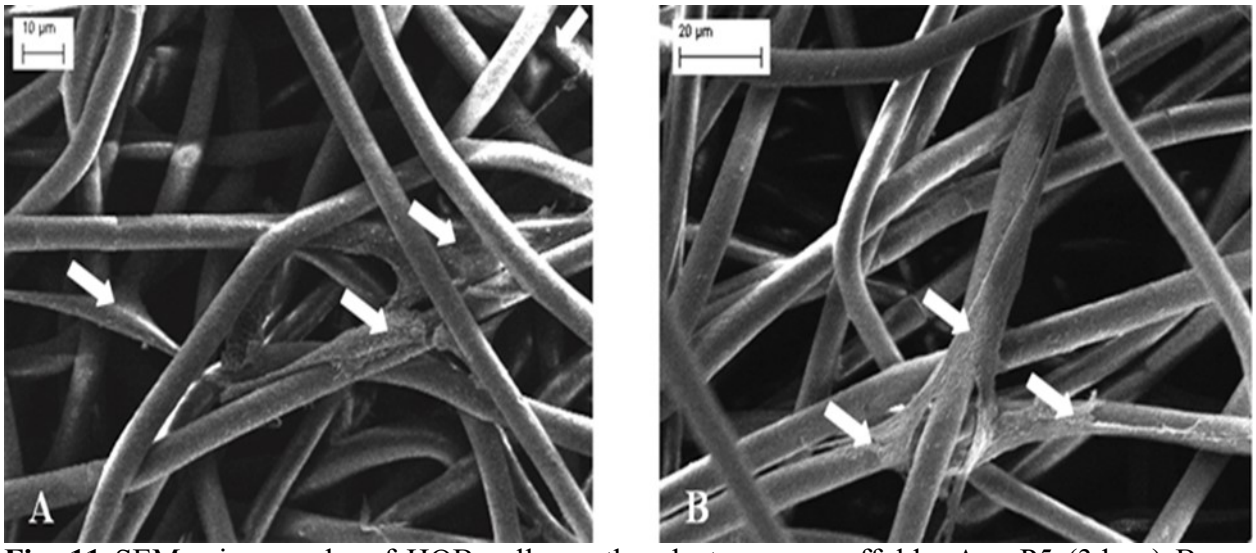

Fig. 11 SEM micrographs of HOB cells on the electrospun scaffolds. A – P5 (3days) B-control P0 (3 days).

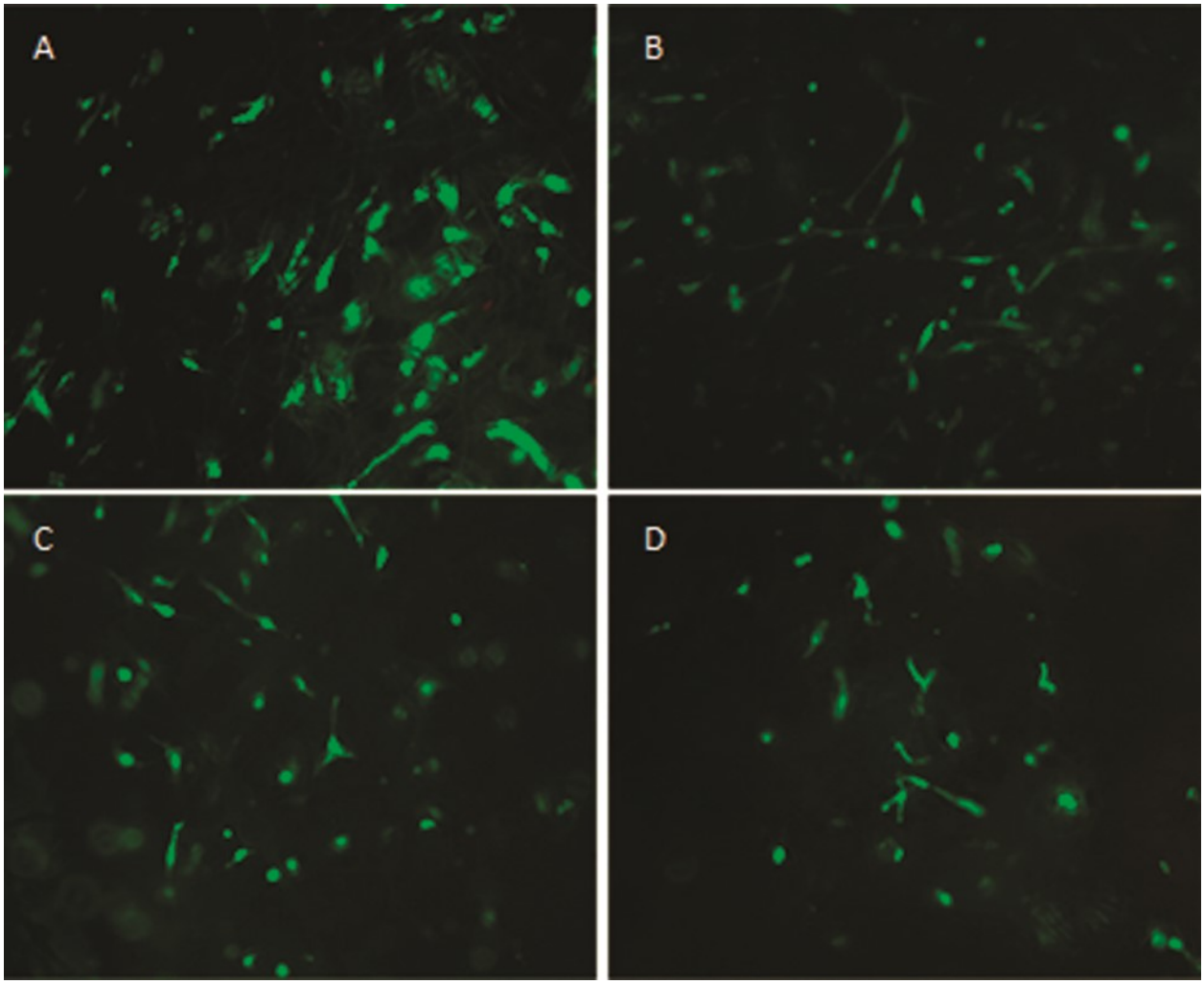

Figure 13 Microscopic micrographs of Live/Dead staining after 1 day (A,C) and 3 days (B,D): A – control P0 (1 day), B- control P0 (3 days), C – P5 (1 day), D - P5 (3 days). Live cells are stained green and dead/damaged cells are stained red (original magnification 10x). (yellow arrow indicates the dead cells visualised in red colour)

4. Conclusions

The requirements for a scaffold for bone tissue engineering include physical stability, suitable degradation profile, and adequate bone cell compatibility. The electrospinning process provides a promising means for creating a tissue-engineered scaffold. In this investigation novel fibrous porous tri-phasic composite membranes were collected and analysed. Nano sized hydroxyapatite was electrospun simultaneously within the polymeric matrix of PHB98-PHV2, with the aid of *Bombyx mori* silk fibroin essence. Silk fibroin, a biodegradable polymer, balanced the change in solution electrospinning dynamic produced

by the presence of nanohydroxyapatite particles while improving fibre deposition. The significance of presence of nHAp within the polymer is its bioactivity. It is established that the presence of Ca_2 stimulates osteoblastic proliferation and depresses osteoclast-mediated bone resorption through negative feedback loops [59, 60]. Furthermore HAp is also known to enhance cell adhesion through an inherently high capacity of adsorbing proteins [60]. The electrospun fibre diameters were found to increase with increased concentration of the co-phases within the polymeric matrix, while the contact angle measurements showed a decrease in wettability even if the values remained within the hydrophilic range (< 90°). The mechanical characterisation showed an increase in Young's modulus for composites containing 2% wt of ceramic and 2%wt of silk fibroin when compared to the pure polymeric matrix. Additionally when further increasing the ceramic and proteic phases concentrations to 5 wt.% the modulus decreases. Compressive tests showed a proportional decrease in compressive secant modulus with increasing ceramic content. Further results confirmed that the composite membranes were bioactive, supporting bone like apatite crystals growth after 28 days. The formation of hydroxyapatite crystals on nanofibrous surfaces provides a suitable topography mimicking the extra cellular matrix while supports and improves osteoblast cell attachment and proliferation *in vivo*. Preliminary *in vitro* biological tests proved that the composite fibrous membranes were biocompatible and supported cell attachment, presenting suitable characteristics for scaffold development. Similarly the cells were able to penetrate into the composite membrane and elongate themselves in the direction of the fibres after 3 days of culture. Future efforts are focused on building a three dimensional composite structure intended for bone tissue regeneration utilising the approach developed in this work.

Acknowledgements

This research has been supported by an IRCSET (Irish Research Council for Science and Technology) EMBARK Initiative Scholarship. The authors also want to thank Maurice Burke, Dr. Joanna Podporska–Carroll and Dr. Rosaleen Devery.

Appendix A. Supplementary data

Supplementary data to this article can be found online at http://dx.doi.org/10.1016/j.msec.2013.08.012.

References

[1] R. Murugan,. S.Ramakrishna, Development of nanocomposites for bone grafting. *Composites Science and Technology,* 65(15–16), (2005), 2385-2406.

[2] S.P. Hoerstrup,, Overview of tissue engineering *IN:* Ratner BD, Hoffman A.S., Schoen F.J., (ed.) *Biomaterial science: an introduction to materials in medicine.* 2nd ed. San Diego Elsevier Academic Press, 2004, pp.712-727.

[3] D. Loca, J. Locs, K. Salma, J. Gulbis, I. Salma, L. Berzina-Cimdina ,. Porous Hydroxyapatite Bioceramic Scaffolds for Drug Delivery and Bone Regeneration, *IN: ICC3: Symposium 13: Ceramics for Medicine, Biotechnology and Biomimetics.* Japan: IOP Conf. Series: Materials Science and Engineering 18, (2008).

[4] R. Vasita, D.S. Katti, Nanofibers and their applications in tissue engineering, *Int J Nanomedicine,* 1(1), (2006),.15-30.

[5] P. D. Dalton, D. Grafahrend, K. Klinkhammer, D. Klee, M. Moller. Electrospinning of polymer melts: Phenomenological observations, *Polymer,* 48, (2007),6823-6833.

[6] M.P. Lutolf, Synthetic biomaterials as instructive extracellular microenvironments for morphogenesis in tissue engineering. *Nat. Biotechnol,* 23, (2005), 47-55.

[7] D. Liang, B.S Hsiao, B. Chu, Functional electrospun nanofibrous scaffolds for biomedical applications, *Adv. Drug Deliv. Rev,* 59 (14), (2007),1392-1412

[8] S. Chakraborty, I-C. Liao, A. Adler, K.W. Leong, Electrodynamics: a facile technique to fabricate drug delivery systems, *Adv. Drug Deliv. Rev,* 61(12), (2009), 1043-1054.

[9] A.M.C Barradas, H. Yuan, C.A van Blitterswijk, P. Habibovic, Osteoinductive Biomaterials: Current Knowledge of Properties, Experimental Models and Biological Mechanisms, *European Cells and Materials,* 21, (2011), 407-429

[10] H. Wang, Y.Li, Y. Zuo, J. Li, S. Ma, L. Cheng, Biocompatibility and osteogenesis of biomimetic nano-hydroxyapatite/polyamide composite scaffolds for bone tissue engineering. *Biomaterials,* 28(22), (2007a), 3338-3348.

[11] E. Fukada, Piezoelectric properties of Poly b-hydroxybutyrate and copolymers of ß-hydroxybutyrate and b-hydroxyvalerate . *Int J Biol Macromol,* 8, (1986.), 361-366.

[12] G.-Q. Chen, The application of polyhydroxyalkanoates as tissue engineering materials, Biomaterials. *Biomaterials,* 26, (2005), 6565-6578.

[13] S. Naznin, Production and Characterization of Tissue Engineering Scaffolds based on Polyhydroxybutyrateco- hydroxyvalerate polymers. *IN: 2012 International Conference on Biomedical Engineering (ICoBE).* Penang, 2012

[14] R.N. Reusch, Low molecular weight complexed poly (3-hydroxybutyrate):a dynamic and versatile molecule in vivo. *Can J Microbiol,* 41, (1995), 50-54.

[15] G. Torun Kose, H. Kenar, N. Hasırcı, V. Hasırcı, Macroporous poly (3-hydroxybutyrate-co-3-hydroxyvalerate) matrices for bone tissue engineering. *Biomaterials,* 24 (11), (2003), 1949-1958.

[16] Y. Wang, X. Wang, K. Wei, N. Zhao, S. Zhang, J. Chen, Fabrication, characterization and long-term in vitro release of hydrophilic drug using PHBV/HA composite microspheres, *Materials Letters,* 61(4–5), (2007b), 1071-1076.

[17] J. Venugopal, M.P. Prabhakaran, Y. Zhang, S. Low, A.T. Choon, S. Ramakrishna, Biomimetic hydroxyapatite-containing composite nanofibrous substrates for bone

tissue engineering. *Philisophical Transactions of the Royal Society A,* 368 (1917), (2010), 2065-2081.

[18] L. Lao, Y. Wang, Y. Zhu, Y. Zhang, C. Gao, Poly(lactide-co-glycolide)/hydroxyapatite nanofibrous scaffolds fabricated by electrospinning for bone tissue engineering. *J Mater Sci: Mater Med,* 22, (2011), 1873-1884

[19] N. Galego, C. Rozsa, R. Sanchez, J. Fung, A. Vazquez, J.S. Tomas, Characterization and application of poly (b-hydroxyalkanoates)family as composite biomaterials, *Polym Test,* 19, (2000), 485-492.

[20] G. H. Altman, F. Diaz, C. Jakuba, T. Calabro, R. L. Horan, J. Chen, H. Lu, J. Richmond, D. L. Kaplan, Silk-based biomaterials. *Biomaterials,* 24, (2003), 401-416.

[21] A.G. Mikos, J.S. Temenoff, Formation of Highly Porous Biodegradable Scaffolds for Tissue Engineering, Electronic Journal of Biotechnology, *Electronic Journal of Biotechnology,* 3(2), (2000), 114-119.

[22] G. Freddi, P. Monti, M. Nagura, Y. Gotoh, M. Tsukada, Structure and molecular conformation of tussah silk fibroin films: effect of heat treatment. *Journal of Polymer Science Part B: Polymer Physics,* 35 (5), (1997), 841-847.

[23] L. Wang, R. Nemoto, M. Senna, Changes in microstructure and physico-chemical properties of hydroxyapatite–silk fibroin nanocomposite with varying silk fibroin content, *Journal of the European Ceramic Society,* 112 (1), (2004), 2707-2715.

[24] K. Fujihara, M. Kotaki, S. Ramakrishna, Guided bone regeneration membrane made of polycaprolactone/calcium carbonate composite nano-fibers, *Biomaterials,* 26 (19), (2005), 139-4147.

[25] H.-W. Kim, J.-H. Song, H.-E. Kim, Nanofiber generation of gelatin–hydroxyapatite biomimetics for guided tissue regeneration, *Adv Funct Mater,* 15 (12), (2005), 1988-1994.

[26] G. Sui, X. Yang, F. Mei, X. Hu, G. Chen, X. Deng, S. Ryu, Poly-l-lactic acid/hydroxyapatite hybrid membrane for bone tissue regeneration. *J Biomed Mater Res, Part A,* (2007), 445-454, DOI: 10.1002/jbm.a.31166

[27] X.L. Deng, G. Sui, M.L. Zhao, G.Q. Chen, Yang X.P., Poly (l-lactic acid)/hydroxyapatite hybrid nanofibrous scaffolds prepared by electrospinning, *J Biomater Sci Polym Ed,* 18 (1), (2007), 117-130,

[28] X. Xu, X. Chen, A. Liu, Z. Hong, X. Jing, Electrospun poly(l-lactide)-grafted hydroxyapatite/poly(l-lactide) nanocomposite fibers, *European Polymer Journal,* 43 (8), (2007), 3187-3196.

[29] S.A. Catledge, W.C. Clem, N. Shrikishen, S. Chowdhury, A.V. Stanishevsky, M. Koopman, Y.K. Vohra, An electrospun triphasic nanofibrous scaffold for bone tissue engineering. *Biomed Mater*, 2 (2), (2007), 142-150.

[30] J. Venugopal, P. Vadgama, T.S.S. Kumar, S Ramakrishna, Biocomposite nanofibres and osteoblasts for bone tissue, *Nanotechnology*, 18, (2007), 1-8.

[31] M.P. Prabhakaran, J. Venugopal, S. Ramakrishna, Electrospun nanostructured scaffolds for bone tissue engineering. *Acta Biomaterialia*, 5 (8), (2009), 2884-2893.

[32] L. Wang, L. Chunzhong, Preparation and physicochemical properties of a novel hydroxyapatite/chitosan–silk fibroin composite*, Carbohydrate Polymers,* 68(4), (2007), 740-745.

[33] D. Guan, Z. Chen, C. Huang, Y. Lin, Attachment, proliferation and differentiation of BMSCs on gas-jet/electrospun nHAP/PHB fibrous scaffolds. *Applied Surface Science,* 255(2), (2008), 324-327.

[34] P.Q. Franco, C.F.C. João, J.C. Silva, J.P. Borges, Electrospun hydroxyapatite fibers from a simple sol–gel system, *Materials Letters,* 67 (1), (2012)*,* 233-236.

[35] Y. Ito, H. Hasuda, M. Kamitakahara, C. Ohtsuki, M. Tanihara, I-K. Kan, O-H. Kwon, A composite of hydroxyapatite with electrospun biodegradable nanofibers as

a tissue engineering material, *Journal of Bioscience and Bioengineering,* 100 (1), (2005), 43-49.

[36] K.C. Remant Bahadur, C.K. Kim, M.S. Khil, H.Y. Kim, I.S. Kim, Synthesis of hydroxyapatite crystals using titanium oxide electrospun nanofibres, *Materials Science and Engineering: C,* 28, (2006), 70-74.

[37] W. Cui, X. Li, C. Xie, H. Zhuang, S. Zhou, J. Weng, Hydroxyapatite nucleation and growth mechanism on electrospun fibers functionalized with different chemical groups and their combinations. *Biomaterials,* 31 (17), (2010), 4620-4629.

[38] M.V Jose, V Thomas, K.T Johnson, D.R Dean, E. Nyalro, Aligned PLGA/HA nanofibrous nanocomposite scaffolds for bone tissue engineering, *Acta Biomater.,* 5, (2009), 305-315.

[39] H.M. Nie, Fabrication and characterization of PLGA/ HAp scaffolds for delivery of BMP-2 plasmid composite DNA, *J Control Release,* 120, 2007), 111-121.

[40] H. Nie, B.W. Soh, Y.C Fu, C.H. Wang, Three-dimensional fibrous PLGA/HAp composite scaffold for BMP-2 delivery, *Biotechnol Bioeng,* 99, (2008), 223-234.

[41] A. Oyane, H.-M. Kim, T. Furuya, T. Kokubo, T. Miyazaki, T. Nakamura, Preparation and assessment of revised simulated body fluids, *Journal of Biomedical Materials Research Part A,* 40 (17), (2003), 188-195.

[42] H.X Yang, M. Sun, Y. Zhang, P. Zhou, Degradable PHBHHx Modified by the Silk Fibroin for the Applications of Cardiovascular Tissue Engineering, *ISRN Materials Science,* vol. 2011, Article ID 389872, (2011),11 pages

[43] V. Konduru, Static and Dynamic Contact Angle Measurement on Rough Surfaces Using Sessile Drop Profile Analysis with Application to Water Management in Low Temperature Fuel Cells, *Michigan Technological University*, 2010, page 27

[44] B. Clarke., Normal Bone Anatomy and Physiology, *Clin J Am Soc Nephrol,* 3, (2008), 131-139.

[45] J. Graham, M Ries, L. Pruitt, Effect of bone porosity on the mechanical integrity of the bone-cement interface, *J Bone Joint Surg Am.,* 85(A), (2003), 1901-1908.

[46] Y. Pan, Preparation and characterization of nano-hydroxyapatite/polyvinyl alcohol gel composites. *Journal of Wuhan University of Technology--Materials Science Edition,* 25, (2010), 474-478.

[47] L. Medvecky, Microstructure and Properties of Polyhydroxybutyrate-Chitosan-Nanohydroxyapatite Composite Scaffolds, *The Scientific World Journal*, Volume 2012, Article ID 537973, (2012), 8pages

[48] J.Y Baek, Z.C. Xing, G. Kwak, K.B. Yoon, S.Y. Park, L.S. Park, I.K Kang, 2Fabrication and Characterization of Collagen-Immobilized Porous PHBV/HA Nanocomposite Scaffolds for Bone Tissue Engineering. *Journal of Nanomaterials*, Volume 2012 , Article ID 171804, (2012),11 pages

[49] J. Wang, F. Yu, L. Qu, X. Meng, G. Wen, Study of synthesis of nano-hydroxyapatite using a silk fibroin template, *Biomedical Materials,* (041002), (2010)

[50] A. Vasconcelos, G. Freddi, A. Cavaco-Paulo, Biodegradable Materials Based on Silk Fibroin and Keratin, *Biomacromolecules*, 9, (2008), 1299–1305

[51] S. Singh, A.K. Mohanty, T. Sugie, Y. Takai, H. Hamada, Renewable resource based biocomposites from natural fiber and polyhydroxybutyrate-co-valerate (PHBV) bioplastic, *Composites Part A: Applied Science and Manufacturing,* 39(5), (2008), 875-886.

[52] C.C. Silva, A. G. Pinheiro, M. A. R. Miranda, J. C. Góes, A. S. B. Sombra, Structural properties of hydroxyapatite obtained by mechanosynthesis, *Solid State Sciences,* 5, (2003), 553-558

[53] G. Penel, G. Leroy, C. Rey, E. Bres, MicroRaman spectral study of the PO_4 and CO_3 vibrational modes in synthetic and biological apatites, *Calcified Tissue International,* 63, (1998), 475-481

[54] E.A Voger, Short-term cell-attachment rates: a surface-sensitive test of cell-substrate compatibility, *J Biomed Mater Res,* 21(10), (1987), 1197-1211.

[55] G.A. Stanciu, I. Sandulescu, B. Savu, S.G Stanciu, K.M. Paraskevopoulos, X. Chatzistavrou, E. Kontonasaki, P. Koidis, Investigation of the Hydroxyapatite Growth on Bioactive Glass Surface, *Journal of Biomedical & Pharmaceutical Engineering*, 1(1), (2007), 34-39

[56] J. E. Kurkijarvi, M. J. Nissi, I. Kiviranta, J. S. Jurvelin, M.T. Nieminen, Delayed gadolinium-enhanced MRI of cartilage (dGEMRIC) and T-2 characteristics of human knee articular cartilage: topographical variation and relationships to mechanical properties, *Magn. Reson. Med,* (52), (2004), 41-46.

[57] A. Kumarasuriyar, L. Grøndahl, V. Nurcombe, S.M. Cool, Osteoblasts up-regulate the expression of extracellular proteases following attachment to Poly(β-hydroxybutyrate-co-β-hydroxyvalerate). *Gene,* 428(1–2), (2009), 53-58.

[58] G.T. Köse, F. Korkusuz, P. Korkusuz, N. Purali, A. Özkul, V. Hasırci, Bone generation on PHBV matrices: an in vitro study. *Biomaterials,* 24(27), (2003), 4999-5007.

[59] M. Zaidi, J. Kerbie, C.L.-H. Huang, A.S.M.T. Alam, H. Rathod, T.J. Chambers, B.S. Moonga, Divalent cations mimic the inhibitory effect of extracellular ionized calcium on bone resorption by isolated rat osteoclasts: further evidence for a ‘‘calcium receptor”, *J Cell Phys*, 149, (1991), 422–427.

[60] Z. Meleti, I.M. Shapiro, C.S. Adams, Inorganic phosphate induces apoptosis of osteoblasts-like cells in culture, *Bone*, 27, (2000),359–366.